OPEN ACCESS
JOURNAL OF ADVANCED DIELECTRICS
Vol. 13, No. 1 (2023) 2242009 (8 pages)

DOI: 10.1142/S2010135X22420097

XI'AN JIAOTONG UNIVERSITY
World Scientific
www.worldscientific.com

A novel $Sr_5BiTi_3Nb_7O_{30}$ tungsten bronze ceramic with high energy density and efficiency for dielectric capacitor applications

Xiangting Zheng[*], Wentao Zhong[*], Peng Zheng[*,‡], Wangfeng Bai[†], Chong Luo[†], Liang Zheng[*] and Yang Zhang[*]

[*]*Lab for Nanoelectronics and NanoDevices, Department of Electronics Science and Technology Hangzhou Dianzi University, Hangzhou 310018, P. R. China*

[†]*College of Materials and Environmental Engineering, Hangzhou Dianzi University, Hangzhou 310018, P. R. China*

[‡]zhengpeng@hdu.edu.cn

Received 25 September 2022; Revised 26 November 2022; Accepted 20 December 2022; Published 31 January 2023

Dielectric capacitors with high capacitive energy storage are urgently needed to meet the growing demand for high-performance energy storage devices. Herein, a novel lead-free $Sr_5BiTi_3Nb_7O_{30}$ (SBTN) tungsten bronze relaxor ferroelectric ceramic is prepared and explored for potential energy storage applications. A high recoverable energy density W_{rec} (~ 3.72 J/cm^3) and ultrahigh efficiency η (~ 94.2%) at 380 kV/cm are achieved simultaneously. Both W_{rec} and η exhibit superior stabilities against temperature (30–140°C), cycles (10^0–10^5) and frequency (1–500 Hz). In addition, a high current density of 796 A/cm^2 and a large power density of 71.7 MW/cm^3 are achieved, together with good thermal endurance and fatigue resistance. These results demonstrate that the obtained SBTN ceramic can be deemed as the promising candidates for dielectric capacitor applications.

Keywords: Energy storage ceramic; tungsten bronze; relaxor ferroelectrics; charge–discharge.

1. Introduction

Rapid developments in modern industry and technology bring about enormous energy and environmental challenges.[1] How to effectively store capacity, reduce capacity loss, and reduce environmental pollution have become urgent problems. Compared to batteries and supercapacitors, dielectric capacitors possess the highest power density, quick charging–discharging speed, excellent cycling stability, wide operating temperature range, and high breakdown resistance.[2–5] Yet, the small energy storage density greatly limits their practical applications.[6,7]

The recoverable energy density (W_{rec}) of dielectric materials is determined by $W_{rec} = \int_{Pr}^{P\max} EdP$, where $P_{\max}$ and P_r denote the maximum and remanent polarization, respectively, and E is the electric field value.[8] Due to the large ΔP ($\Delta P = P_{\max} - P_r$), lead-based perovskite antiferroelectrics (AFEs) and relaxor ferroelectrics (RFEs) usually exhibit a high W_{rec} and large efficiency (η). However, the international restrictions on the use of lead-containing materials inspire the research interest in lead-free materials. Up to now, various lead-free energy storage materials with high energy storage performances (ESPs) are mainly focused on the perovskite ferroelectrics including $BaTiO_3$ (BT)-based,[9–13] $(Bi_{0.5}K_{0.5})TiO_3$ (BKT)-based,[14–18] $(Bi_{0.5}Na_{0.5})TiO_3$ (BNT)-based,[19–23] $(Sr_{0.7}Bi_{0.2})TiO_3$ (SBT)-based,[24–28] $NaNbO_3$ (NN)-based, $AgNbO_3$ (AN)-based ceramics.[29–32] Despite a lot of excellent achievements, the ESP of the lead-free perovskite ferroelectrics still needs to meet the practical application requirements. Compared to the widely studied perovskite lead-free ferroelectrics, tungsten bronze (TB)-based lead-free ferroelectrics are seldom involved, which are deemed as the second large category of the ferroelectric family. Recently, Cao *et al.* introduced Gd^{3+} into $Sr_2NaNb_5O_{15}$ TB ceramic, in which a W_{rec} (~ 2.37 J/cm^3) and a large η (~ 94.4%) were realized.[33] A high W_{rec} of 3.23 J/cm^3 and a high η of 88.2% were achieved concurrently under 290 kV/cm in a $Sr_{1.75}Ca_{0.25}NaNb_5O_{15}$ TB ceramic.[34] All these works mean that TB-based lead-free ferroelectrics also possess enormous potential in the energy storage field, which deserves more research attention.

Notably, similar to Pb^{2+} ions with lone pair electron configuration, the hybridization between Bi^{3+} 6p and O^{2-} 2p orbitals is strongly strengthened, which is conductive to maintain large $P_{\max}$. Furthermore, the B-site which possesses different ionic valence and radii can effectively produce polar nanoregions (PNRs) that initiate relaxation properties, thus potentially generating a moderate dielectric constant, low P_r, and high W_{rec}.[22] Herein, a novel lead-free $Sr_5BiTi_3Nb_7O_{30}$ TB-based ceramic is designed for energy storage applications.

[‡]Corresponding author.

Crystal structures, microstructures, dielectric and ferroelectric properties are discussed in detail. A large W_{rec} (~3.72 J/cm^3), ultrahigh η (~94.2%), a high power density (P_D = 71.7 MW/cm^3), and an extremely fast discharge rate ($\tau_{0.9}$ < 60 ns) are realized simultaneously, which are superior to most recently reported TB structural ceramics.

2. Experimental Procedures

The $Sr_5BiTi_3Nb_7O_{30}$ (SBTN) ceramic was manufactured via the conventional solid-state method. $SrCO_3$ (99.5%, Aladdin), Bi_2O_3 (99.5%, Shudu Nanomaterials), TiO_2 (99.8%, Zhongxing Electronic Materials) and Nb_2O_5 (99.5%, SCR) were selected as the raw materials, and then these powders were weighed and mixed by ball milling for 12 h. After drying, the mixtures were calcined under 1100°C for 2 h, and then the obtained powders were pressed into disks with a diameter of 12 mm. Finally, the disks were heated to 550°C for 2 h to remove PVA, and then sintered under 1275°C for 3 h.

A MiniFlex600 (Rigaku, Japan) X-ray diffraction and a Horiba/Jobin Yvon Raman spectra (Villeneuve d'Ascq, France) with 532 nm excitation were adopted to judge the phase structure. A JEOL JSM7800 scanning electron microscope (JEOL JSM6460-LV) was employed to observe the microstructure. The band gap (E_g) of the ceramic was determined by a TU-1901 UV–Vis spectrophotometer (Puxi Instruments Technology, China). A Keysight E4990A Impedance analyzer was used to characterize the dielectric properties with respect to temperature and frequency. The ferroelectric properties were tested with a RT1-Premier II ferroelectric analyzer (Radiant Technologies Inc., USA). A CFD-003 charge–discharge instrument (Gogo Instruments Technology, China) was used to measure the energy release behavior of the ceramic capacitor.

3. Results and Discussion

Figure 1(a) exhibits XRD pattern for the SBTN ceramic, in which a unitary TB structure without any apparent secondary phase can be determined according to the PDF card (# 38-1250). To further confirm the phase structure of the ceramic, the Raman spectrum is collected and deconvoluted to distinguish the Raman vibrational modes, as plotted in Fig. 1(b). The Raman spectra falls into three characteristic peaks of 260, 605 and 845 cm^{-1}, which are associated with the internal BO_6 octahedral vibrations.[35] The broadened Raman vibrational modes demonstrate a high degree of site disorder, which might interrupt the long-range ferroelectric order and induce a relaxor behavior.[8]

Figure 1(c) gives the surface structure of the SBTN ceramic, in which a compact structure with no obvious holes can be observed. The EDS and mapping results of the ceramic are also shown in Figs. 1(d) and 1(e). All the elements are uniformly dispersed in the ceramic, which means the formation of a solid solution. A slight composition deviation can be observed, probably due to the Bi volatilization during the high-temperature sintering process.

Figure 2(a) displays the temperature-dependent dielectric constant and loss for the SBTN sample. Frequency dispersion can be observed, indicating a relaxor behavior. To further evaluate the relaxation degree of the ceramics, the modified

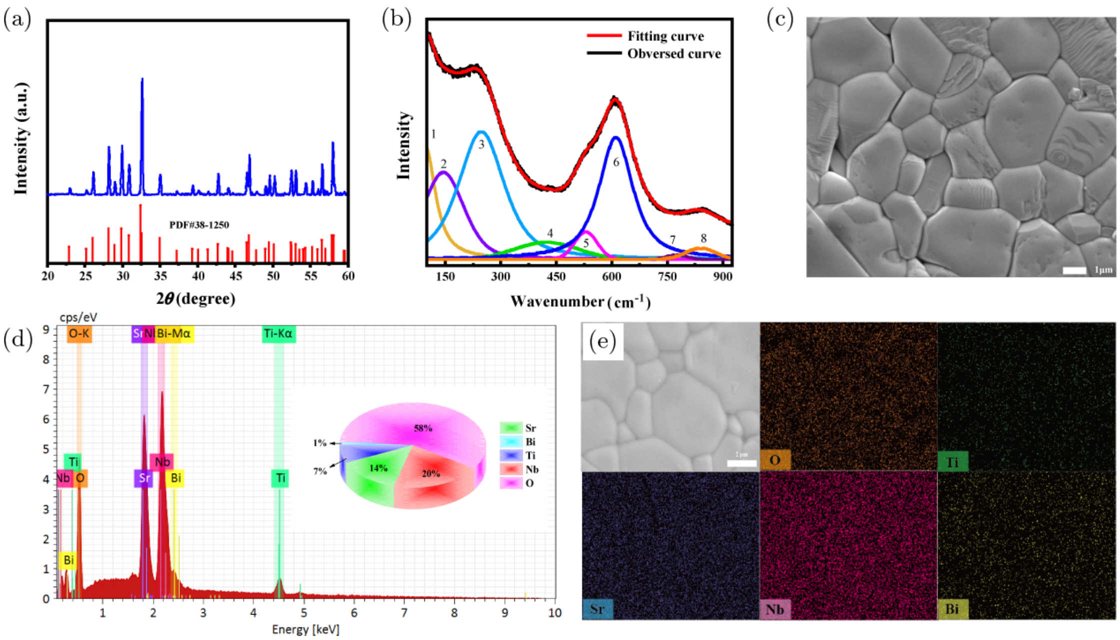

Fig. 1. (a) XRD pattern, (b) Raman spectra, (c) microscopic surface morphology, (d) EDS analysis, and (e) elemental mapping for the SBTN sample.

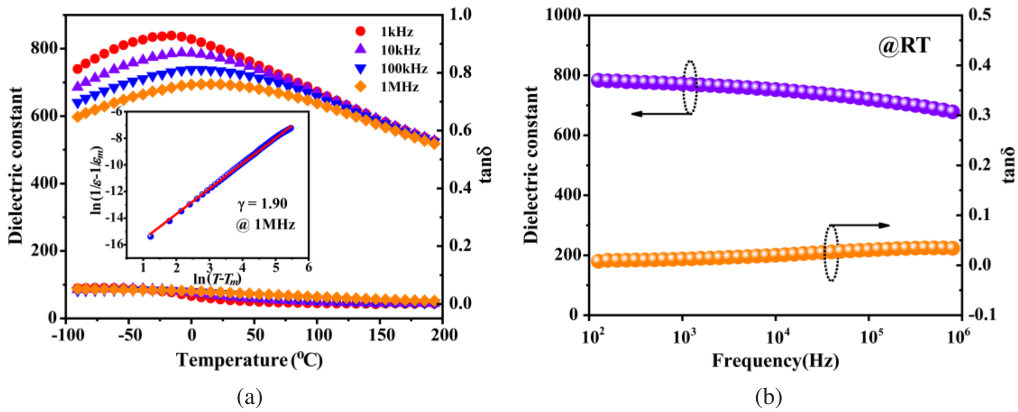

Fig. 2. (a) Temperature- and (b) frequency- dependent dielectric response for the SBTN ceramic, the *inset* of Fig. 2(a) gives a plot of ln(1/ε_r–1/ε_m) as a function of ln(T–T_m) for SBTN ceramic at the frequency of 1 MHz.

Curie–Weiss law ($\frac{1}{\varepsilon_r}-\frac{1}{\varepsilon_m}=\frac{(T-T_m)^\gamma}{C}$ (at $T > T_m$)) was introduced, where ε_m denotes the maximum dielectric constant, C denotes the Curie-like constant, γ corresponds to the relaxation degree constant, and T_m is the corresponding temperature at the maximum permittivity value. Notably, a high value of γ (~1.90) was obtained, indicating a strong relaxation. Figure 2(b) shows the frequency-dependent dielectric properties for the SBTN ceramic over the frequency range from 100 MHz to 1 MHz at room temperature, in which frequency-stable dielectric permittivity and loss can be seen. Note that the modest dielectric constant can guarantee high $P_{\max}$ and relatively large dielectric breakdown strength (E_b). Furthermore, the low dielectric loss can effectively reduce the heat generation during charge–discharge process, producing highly thermal stability.[36]

The bipolar P–E loop and the corresponding electric field–current (I–E) curve at fixed 140 kV/cm for the ceramic are shown in Fig. 3(a). The I–E curve of SBTN ceramic shows negligible domain switching-induced current peaks,

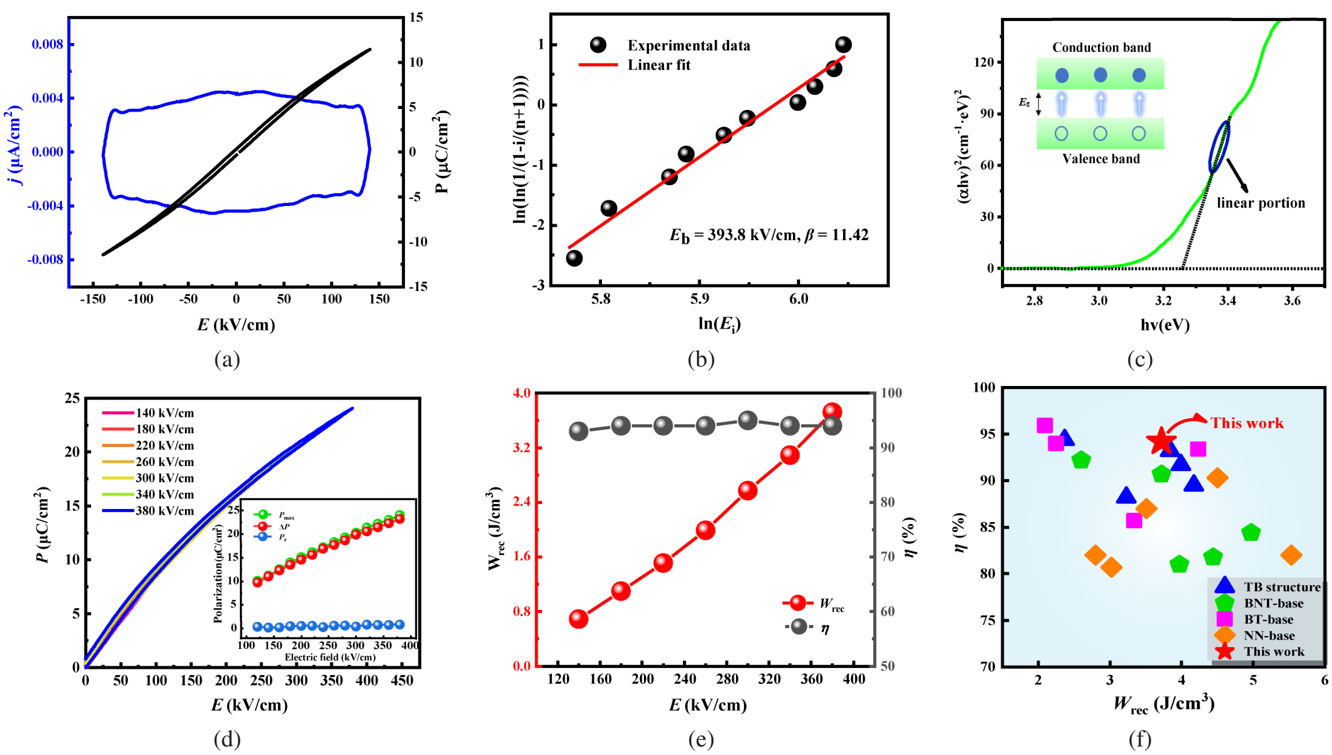

Fig. 3. (a) Bipolar and electric field–current curve, (b) Weibull distribution, (c) plot of $(\alpha h\nu)^2$ versus $h\nu$, (d) unipolar P–E loops under various electric fields, the *inset* shows the change of $P_{\max}$, P_r, ΔP, (e) the W_{rec} and η with increasing applied fields for SBTN ceramic, and (f) comparison of the ESP of SBTN and other energy storage materials.

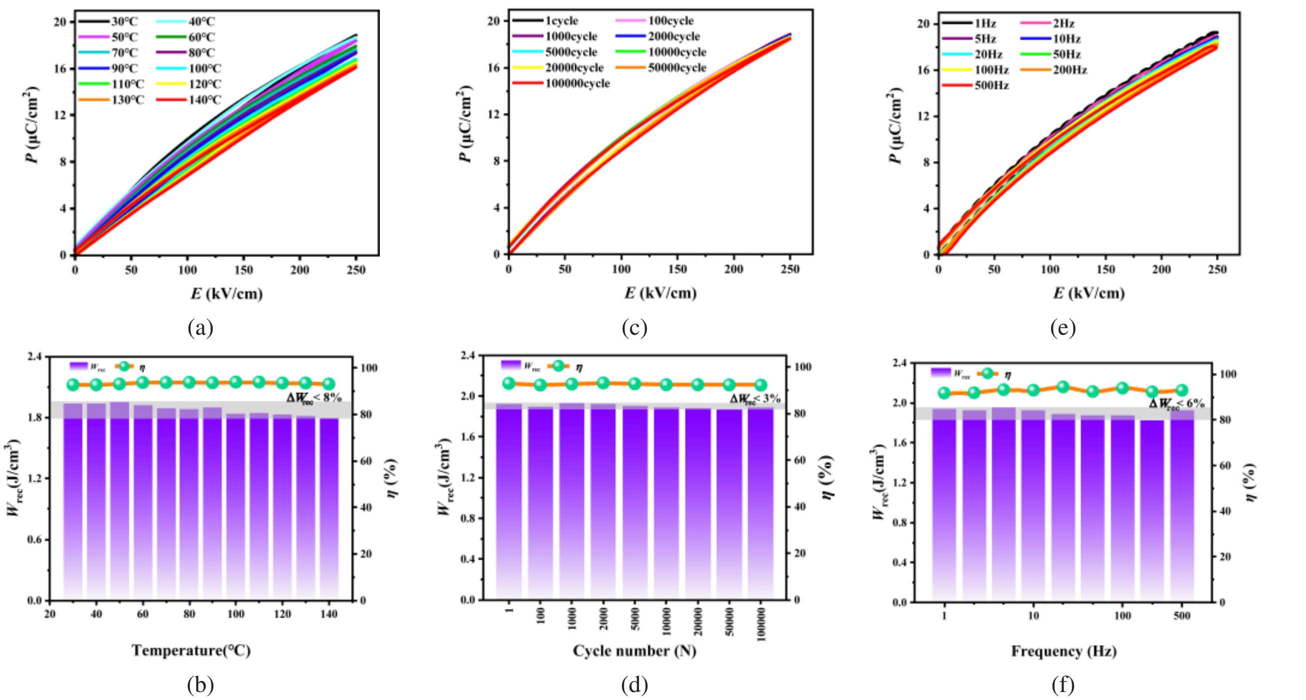

Fig. 4. Unipolar *P–E* loops as functions of (a) temperature, (c) cycles, and (e) frequency. The variations of W_{rec} and η with respect to (b) temperature, (d) cycles, and (f) frequency for SBTN ceramic.

which indicates that the long-range ferroelectric order is interrupted, giving rise to PNRs.[37] Thus, a slim bipolar *P–E* loop with negligible P_r can be observed, consistent with its relaxor nature. The E_b of the SBTN ceramic analyzed by the Weibull distribution is shown in Fig. 3(b). An average E_b value of 393.8 kV/cm is determined coupled with high reliability ($\beta = 11.42$).[38] By extending the linear portion of the curve to the $h\nu$-axis as shown in Fig. 3(c), a high E_g of 3.26 eV is attained for the SBTN ceramic, which offers the basis for the production of high E_b value.[39]

To estimate the ESP of the SBTN ceramic, the field-dependent *P–E* loops are presented in Fig. 3(d). Apparently, P_{max} increases monotonously, while P_r presents an insignificant variation, giving rise to an increased ΔP from 9.8 μC/cm^2 to 23.2 μC/cm^2 following the field from 120 kV/cm to 380 kV/cm. The values of corresponding W_{rec} and η are shown in Fig. 3(e), in which a continuously increased W_{rec} accompanied by a stable η can be observed. Ultimately, a high W_{rec} of 3.72 J/cm^3 and an ultrahigh η of 94.2% are gained concurrently under 380 kV/cm. The ESP between the present work and some representative lead-free materials reported in recent years is compared in Fig. 3(f).[13,23,33,34,44–57] Apparently, the ESP of this work is superior to most recently reported tungsten bronze structure ceramics.

Figure 4(a) depicts the *P–E* loops at various temperatures from 30°C to 140°C, measured at fixed electric field of 250 kV/cm. It is obvious that the SBTN ceramic maintains a slim *P–E* loop in the whole temperature scope. The values of P_{max} decrease from 18.6 μC/cm^2 to 16.2 μC/cm^2 with increasing temperature, while the values of P_r decrease slightly, which is attributed to the slightly decreased dielectric constant with temperatures (see Fig. 2(a)).[58] Consequently, the W_{rec} value fluctuates by less than 8%, and the η value floats slightly when the temperature rises from 30°C to 140°C, as shown in Fig. 4(b), demonstrating that the SBTN ceramic possesses excellent thermal stability. Figure 4(c) shows the *P–E* curves with increasing cycle numbers. It can be seen that the curves remain slim over the whole fatigue numbers. The corresponding W_{rec} remains almost unchanged, featured by slightly decrease from 1.92 J/cm^3 to 1.87 J/cm^3 with less than 3% change after 10^5 cycles, as shown in Fig. 4(d). This reveals an outstanding fatigue endurance in as-designed ceramic. Furthermore, the frequency-dependent *P–E* curves are also studied, as depicted in Fig. 4(e). Similar slender *P–E* curves can also be found in the frequency range from 1 Hz to 500 Hz. Correspondingly, the values of P_{max} and P_r decrease marginally with increasing frequency, which is a result of the declined dielectric constant with frequency (see Fig. 2(b)). Even so, the values of W_{rec} exhibit a variation of less than 6% over the whole measuring frequency, implying a good frequency resistance (Fig. 4(f)).

The underdamped discharge current curves at various fields and room temperature are plotted in Fig. 5(a). The maximum current (I_{max}), current density ($C_D = I_{max}/S$, S means the electrode area), and power density ($P_D = E \cdot I_{max}/2S$) are shown in Fig. 5(b).[59] Following the enhancement of electric field from 20 kV/cm to 180 kV/cm, the corresponding I_{max} rises from 3.2 A to 25.1 A. Meanwhile, the corresponding C_D and

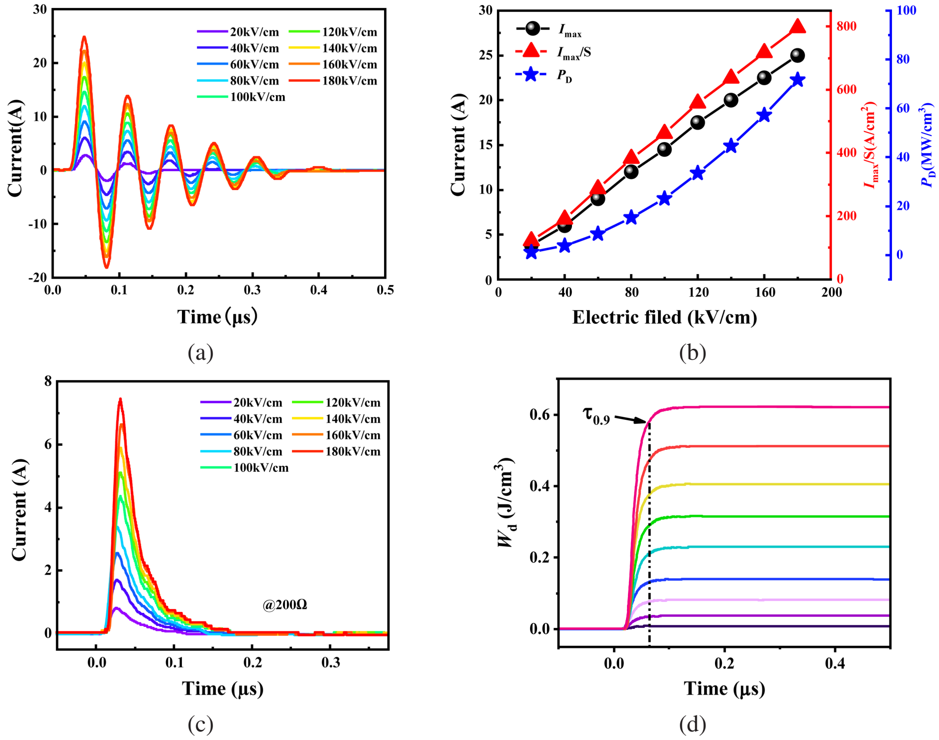

Fig. 5. (a) The underdamped discharge curves and (b) values of I_{max}, C_D, and P_D of the SBTN ceramic with increasing applied electric field. (c) The overdamped discharge curves and (d) the W_d–t loops at different electric fields.

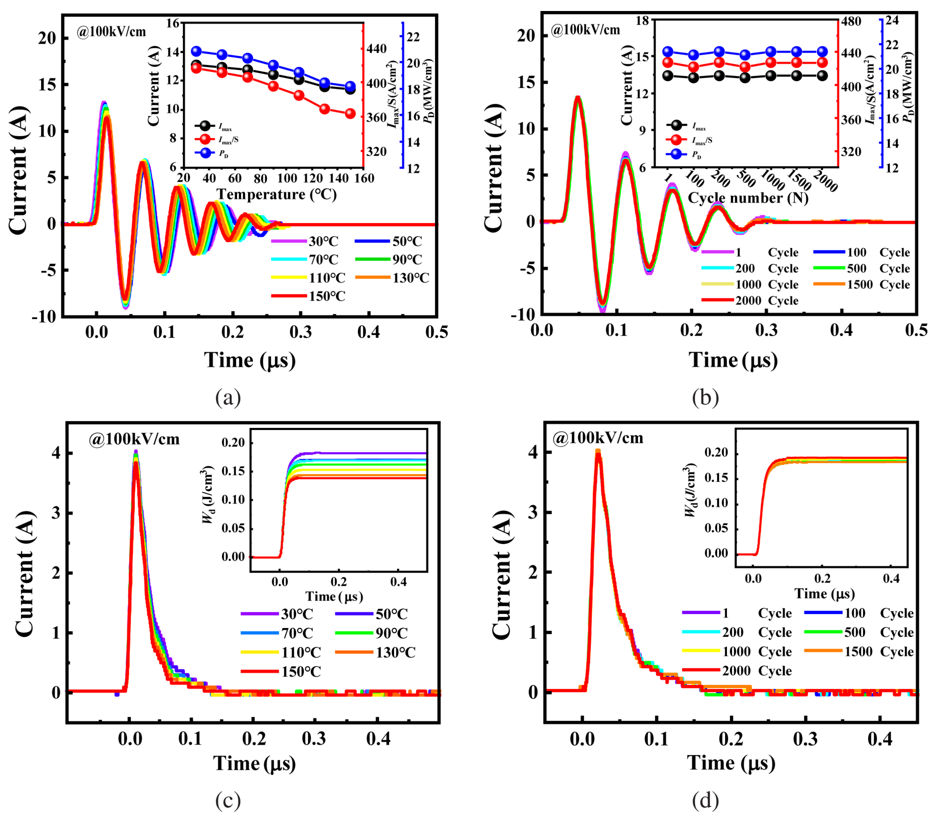

Fig. 6. Underdamped pulse discharge current curves as functions of (a) temperature and (b) cycles. Overdamped pulse discharge current curves with respect to (c) temperature and (d) cycles for the SBTN sample.

P_D obtain the maximum values of 796 A/cm^2 and 71.7 MW/cm^3. Field-dependent overdamped discharge current curves are given in Fig. 5(c), and the calculated discharge energy density (W_d)–t curves are also shown in Fig. 5(d). The discharge time ($\tau_{0.9}$, the time for W_d to decrease 10%) remains less than 60 ns at all tested electric fields, which indicates a terrific fast discharge capability.[60] At 180 kV/cm, the W_d obtains the maximum value of 0.62 J/cm^3.

Figures 6(a) and 6(b) give pulsed underdamped discharge current of the SBTN ceramic in a broad temperature scope of 30–150°C and cycle number range of 1–2000 at a field of 100 kV/cm, respectively. Meanwhile, the corresponding values of $I_{\max}$, C_D and P_D are inserted in Fig. 6(a). With the enhancement of temperature from 30°C to 150°C, a slight drop in peak current can be noticed, and the values of C_D and P_D gradually decrease from 416.5 A/cm^2 and 20.8 MW/cm^3 to 363.4 A/cm^2 and 18.2 MW/cm^3 (the *inset* of Fig. 6(a)). As shown in Fig. 6(b), an excellent fatigue resistance is achieved in the ceramic, characterized by almost no change in P_D and C_D after 2000 cycles. Figures 6(c) and 6(d) plot pulsed overdamped discharge current against temperature and cycles for the SBTN ceramic. The *insets* of Figs. 6(c) and 6(d) plot the W_d–t curves under 100 kV/cm. The overdamped discharge current appears to be slightly reduced, and hence the W_d shows a reduction with increasing temperature. This may be caused by the exacerbation of space charge aggregation as the temperature increases.[16] As given in Fig. 6(d), the indicated ceramic exhibits excellent stability with less than 3% variation of W_d after 2000 cycles.

4. Conclusions

In summary, a novel TB-based lead-free $Sr_5BiTi_3Nb_7O_{30}$ ceramics were designed for dielectric energy storage capacitor applications. An ultrahigh η of 94.2% and a high $W_{\rm rec}$ of 3.72 J/cm^3 are achieved concurrently in as-designed TB ceramic, together with good temperature stability (30–140°C), superior frequency resistance (1–500 Hz), and outstanding fatigue endurance (10^0–10^5). Moreover, the designed ceramic also exhibits an excellent pulsed charging–discharging performance, featured by a fast discharge rate ($\tau_{0.9}$ < 60 ns), high C_D (796 A/cm^2) and large P_D (71.7 MW/cm^3). In addition, the achieved pulsed charging–discharging performance also behaves acceptable thermal stability and remarkable cycling reliability. These achievements suggest that the novel lead-free $Sr_5BiTi_3Nb_7O_{30}$ TB-based ceramics possess huge application potential for future dielectric energy storage applications.

Acknowledgment

This work was supported by the Natural Science Foundation of Zhejiang Province (LY22E020006).

References

[1] Q. Li, L. Chen, M. R. Gadinski, S. Zhang, G. Zhang, U. Li, E. Iagodkine, A. Haque, L. Q. Chen, N. Jackson and Q. Wang, Flexible high-temperature dielectric materials from polymer nanocomposites, *Nature* **523**(7562), 576 (2015).

[2] C. W. Ahn, C. H. Hong, B. Y. Choi, H. P. Kim, H. S. Han, Y. H. Hwang, W. Jo, K. Wang, J. F. Li, J. S. Lee and Ill. W. Kim, A brief review on relaxor ferroelectrics and selected issues in lead-free relaxors, *J. Korean Phys. Soc.* **68**(12), 1481 (2016).

[3] G. Liu, Y. Li, B. Guo, M. Y. Tang, Q. Li, J. Dong, L. J. Yu, K. Yu, Y. Yan, D. W. Wang, L. Y. Zhang, H. B. Zhang, Z. B. He and L. Jin, Ultrahigh dielectric breakdown strength and excellent energy storage performance in lead-free barium titanate-based relaxor ferroelectric ceramics via a combined strategy of composition modification, viscous polymer processing, and liquid-phase sintering, *Chem. Eng. J.* **398** (2020).

[4] L. T. Yang, X. Kong, F. Li, H. Hao, Z. X. Cheng, H. X. Liu, J. F. Li and S. J. Zhang, Perovskite lead-free dielectrics for energy storage applications, *Prog. Mater. Sci.* **102**, 72 (2019).

[5] Z. Yao, Z. Song, H. Hao, Z. Yu, M. Cao, S. Zhang, M. T. Lanagan and H. Liu, Homogeneous/inhomogeneous-structured dielectrics and their energy-storage performances, *Adv. Mater.* **29**(20) (2017).

[6] Q. Li, F. Z. Yao, Y. Liu, G. Z. Zhang, H. Wang and Q. Wang, High-temperature dielectric materials for electrical energy storage, *Annu. Rev. Mater. Sci.* **48**(1), 219 (2018).

[7] Z. T. Yang, F. Gao, H. L. Du, L. Jin, L. L. Yan, Q. Y. Hu, Y. Yu, S. B. Qu, X. Y. Wei, Z. Xu and Y. J. Wang, Grain size engineered lead-free ceramics with both large energy storage density and ultrahigh mechanical properties, *Nano Energy* **58**, 768 (2019).

[8] T. D. Zhang, W. L. Li, Y. Zhao, Y. Yu and W. D. Fei, High energy storage performance of opposite double-heterojunction ferroelectricity-insulators, *Adv. Funct. Mater.* **28**(10) (2018).

[9] F. Li, M. X. Zhou, J. W. Zhai, B. Shen and H. R. Zeng, Novel barium titanate based ferroelectric relaxor ceramics with superior charge–discharge performance, *J. Eur. Ceram. Soc.* **38**(14), 4646 (2018).

[10] W. B. Li, D. Zhou, L. X. Pang, R. Xu and H. H. Guo, Novel barium titanate based capacitors with high energy density and fast discharge performance, *J. Mater. Chem. A* **5**(37), 19607 (2017).

[11] M. Wei, J. H. Zhang, K. T. Wu, H. W. Chen and C. R. Yang, Effect of $BiMO_3$ (M=Al, In, Y, Sm, Nd, and La) doping on the dielectric properties of $BaTiO_3$ ceramics, *Ceram. Int.* **43**(13), 9593 (2017).

[12] L. W. Wu, X. H. Wang and L. T. Li, Lead-free $BaTiO_3$-$Bi(Zn_{2/3}Nb_{1/3})O_3$ weakly coupled relaxor ferroelectric materials for energy storage, *RSC Adv.* **6**(17), 14273 (2016).

[13] M. X. Zhou, R. H. Liang, Z. Y. Zhou and X. L. Dong, Combining high energy efficiency and fast charge–discharge capability in novel $BaTiO_3$-based relaxor ferroelectric ceramic for energy-storage, *Ceram. Int.* **45**(3), 3582 (2019).

[14] P. Jaita, P. Jarupoom, R. Yimnirun, G. Rujijanagul and D. P. Cann, Phase transition and tolerance factor relationship of lead-free $(Bi_{0.5}K_{0.5})TiO_3$-$Bi(Mg_{0.5}Ti_{0.5})O_3$ piezoelectric ceramics, *Ceram. Int.* **42**(14), 15940 (2016).

[15] Z. Pan, Q. Wang, J. Chen, C. Liu, L. L. Fan, L. J. Liu, L. Fang, X. R. Xing and D. Viehland, Enhanced piezoelectric properties of tetragonal $(Bi_{1/2}K_{1/2})TiO_3$ lead-free ceramics by substitution of pure Bi-based $Bi(Mg_{2/3}Nb_{1/3})O_3$, *J. Am. Ceram. Soc.* **98**(1), 104 (2015).

[16] M. Shiga, M. Hagiwara and S. Fujihara, $(Bi_{1/2}K_{1/2})TiO_3$-$SrTiO_3$ solid-solution ceramics for high-temperature capacitor applications, *Ceram. Int.* **46**(8), 10242 (2020).

[17] L. Zheng, Z. A. Niu, P. Zheng, K. Zhang, C. Luo, J. J. Zhang, N. N. Wang, W. F. Bai and Y. Zhang, Simultaneously achieving high energy storage performance and remarkable thermal

stability in $Bi_{0.5}K_{0.5}TiO_3$-based ceramics, *Mater. Today Energy* **28** (2022).

[18]Z. A. Niu, P. Zheng, Y. M. Xiao, C. Luo, K. Zhang, J. J. Zhang, L. Zheng, Y. Zhang and W. F. Bai, Simultaneously achieving high energy storage performance and remarkable thermal stability in $Bi_{0.5}K_{0.5}TiO_3$-based ceramics, *Mater. Today Chem.* **24** (2022).

[19]Y. H. Wan, L. Tang, X. Y. Dang, P. R. Ren, M. Ma, K. X. Song and G. Y. Zhao, High temperature dielectrics based on $Bi_{1/2}Na_{1/2}TiO_3$-$BaTiO_3$-$Sr_{0.53}Ba_{0.47}Nb_2O_6$ ceramics with high dielectric permittivity and wide operational temperature range, *Ceram. Int.* **45**(2), 2596 (2019).

[20]F. Yan, K. W. Huang, T. Jiang, X. F. Zhou, Y. J. Shi, G. L. Ge, B. Shen and J. W. Zhai, Significantly enhanced energy storage density and efficiency of BNT-based perovskite ceramics via A-site defect engineering, *Energy Stor. Mater.* **30**, 392 (2020).

[21]X. Y. Zhao, W. F. Bai, Y. Q. Ding, L. J. Wang, S. T. Wu, P. Zheng, P. Li and J. W. Zhai, Enhancement of recoverable energy density and efficiency of lead-free relaxor-ferroelectric BNT-based ceramics, *J. Eur. Ceram. Soc.* **40**(13), 4475 (2020).

[22]Y. Q. Ding, J. K. Liu, C. Y. Li, W. F. Bai, S. T. Wu, P. Zheng, J. J. Zhang and J. W. Zhai, Tailoring high energy density with superior stability under low electric field in novel $(Bi_{0.5}Na_{0.5})TiO_3$-based relaxor ferroelectric ceramics, *Chem. Eng. J.* **426** (2021).

[23]X. Zhang, D. Hu, Z. B. Pan, X. J. Lv, Z. Y. He, F. Yang, P. Li, J. J. Liu and J. W. Zhai, High capacitive performance at moderate operating field in $(Bi_{0.5}Na_{0.5})TiO_3$-based dielectric ceramics via synergistic effect of site engineering strategy, *Chem. Eng. J.* **406** (2021).

[24]C. W. Cui, Y. P. Pu, Z. Y. Gao, J. Wan, Y. S. Guo, C. Y. Hui, Y. R. Wang and Y. F. Cui, Structure, dielectric and relaxor properties in lead-free ST-NBT ceramics for high energy storage applications. *J. Alloys Compd.* **711**, 319 (2017).

[25]A. Jan, H. X. Liu, H. Hao, Z. H. Yao, M. Emmanuel, W. G. Pan, A. Ullah, A. Manan, A. Ullah, M. H. Cao and A. S. Ahmad, Enhanced dielectric breakdown strength and ultra-fast discharge performance of novel $SrTiO_3$ based ceramics system, *J. Alloys Compd.* **830** (2020).

[26]J. Xie, H. Hao, H. X. Liu, Z. H. Yao, Z. Song, L. Zhang, Q. Xu, J. Q. Dai and M. H. Cao, Dielectric relaxation behavior and energy storage properties of Sn modified $SrTiO_3$ based ceramics, *Ceram. Int.* **42**(11), 12796 (2016).

[27]H. B. Yang, F. Yan, Y. Lin and T. Wang, Novel strontium titanate-based lead-free ceramics for high-energy storage applications, *ACS Sustain. Chem. Eng.* **5**(11), 10215 (2017).

[28]H. B. Yang, F. Yan, Y. Lin and T. Wang, Improvement of dielectric and energy storage properties in $SrTiO_3$-based lead-free ceramics, *J. Alloys Compd.* **728**, 780 (2017).

[29]N. N. Luo, K. Han, M. J. Cabral, X. Z. Liao, S. J. Zhang, C. Z. Liao, G. Z. Zhang, X. Y. Chen, Q. Feng, J. F. Li and Y. Z. Wei, Constructing phase boundary in $AgNbO_3$ antiferroelectrics: Pathway simultaneously achieving high energy density and efficiency. *Nat. Commun.* **11**, 4824 (2020).

[30]Z. L. Lu, W. C. Bao, G. Wang, S. K. Sun, L. H. Li, J. L. Li, H. J. Yang, H. F. Ji, A. Feteira, D. J. Li, F. F. Xu, A. K. Kleppe, D. W. Wang, S. Y. Liu and I. M. Reaney, Mechanism of enhanced energy storage density in $AgNbO_3$-based lead-free antiferroelectrics. *Nano Energy.* **79**, 105423 (2021).

[31]W. W. Yang, H. R. Zeng, F. Yan, J. F. Lin, G. L. Ge, Y. B. Cao, W. T. Du, K. Y. Zhao, G. R. Li, H. J. Xie and J. W. Zhai, Superior energy storage properties in $NaNbO_3$-based ceramics *via* synergistically optimizing domain and band structures, *J. Mater. Chem. A* **10**, 11613 (2022).

[32]H. Qi, R. Z. Zuo, A. W. Xie, A. Tian, J. Fu, Y. Zhang and S. J. Zhang, Ultrahigh energy-storage density in $NaNbO_3$-based lead-free relaxor antiferroelectric ceramics with nanoscale domains, *Adv. Funct. Mater.* **29**, 1903877 (2019).

[33]L. Cao, Y. Yuan, X. Meng, E. Li and B. Tang, Ferroelectric-relaxor crossover and energy storage properties in $Sr_2NaNb_5O_{15}$-based tungsten bronze ceramics, *ACS Appl. Mater. Interfaces* **14**(7), 9318 (2022).

[34]X. Z. Zhang, W. B. Ye, X. Y. Bu, P. Zheng, L. L. Li, F. Wen, W. F. Bai, L. Zheng and Y. Zhang, Remarkable capacitive performance in novel tungsten bronze ceramics, *Dalton Trans.* **50**(1), 124 (2021).

[35]X. L. Zhu, X. M. Chen, X. Q. Liu and X. G. Li, Ferroelectric phase transition and low-temperature structure fluctuations in Ba4Nd2Ti4Nb6O30 tungsten bronze ceramics, *J. Appl. Phys.* **105**(12), 6 (2009).

[36]H. Pan, J. Ma, J. Ma, Q. Zhang, X. Liu, B. Guan, L. Gu, X. Zhang, Y. J. Zhang, L. Li, Y. Shen, Y. H. Lin and C. W. Nan, Giant energy density and high efficiency achieved in bismuth ferrite-based film capacitors via domain engineering, *Nat. Commun.* **9**(1), 1813 (2018).

[37]F. Li, X. Hou, T. Y. Li, R. J. Si, C. C. Wang and J. W. Zhai, Fine-grain induced outstanding energy storage performance in novel $Bi_{0.5}K_{0.5}TiO_3$-$Ba(Mg_{1/3}Nb_{2/3})O_3$ ceramics via a hot-pressing strategy, *J. Mater. Chem. C* **7**(39), 12127 (2019).

[38]L. Zheng, P. C. Sun, P. Zheng, W. F. Bai, L. L. Li, F. Wen, J. J. Zhang, N. N. Wang and Y. Zhang, Significantly tailored energy-storage performances in $Bi_{0.5}Na_{0.5}TiO_3$-$SrTiO_3$-based relaxor ferroelectric ceramics by introducing bismuth layer-structured relaxor BaBi2Nb2O9 for capacitor application, *J. Mater. Chem. C* **9**(15), 5234 (2021).

[39]D. Li, Y. Lin, Q. B. Yuan, M. Zhang, L. Ma and H. B. Yang, A novel lead-free $Na_{0.5}Bi_{0.5}TiO_3$-based ceramic with superior comprehensive energy storage and discharge properties for dielectric capacitor applications, *J. Materiomics* **6**(4), 743 (2020).

[40]F. Li, J. W. Zhai, B. Shen, X. Liu and H. R. Zeng, Simultaneously high-energy storage density and responsivity in quasi-hysteresis-free Mn-doped $Bi_{0.5}Na_{0.5}TiO_3$-$BaTiO_3$-$(Sr_{0.7}Bi_{0.2}\square_{0.1})TiO_3$ ergodic relaxor ceramics, *Mater. Res. Lett.* **6**(7), 345 (2018).

[41]H. Qi, A. W. Xie, A. Tian and R. Z. Zuo, Superior energy-storage capacitors with simultaneously giant energy density and efficiency using nanodomain engineered $BiFeO_3$-$BaTiO_3$-$NaNbO_3$ lead-free bulk ferroelectrics, *Adv. Energy Mater.* **10**(6) (2019).

[42]J. P. Shi, X. L. Chen, X. Li, J. Sun, C. C. Sun, F. H. Pang and H. F. Zhou, Realizing ultrahigh recoverable energy density and superior charge–discharge performance in $NaNbO_3$-based lead-free ceramics via a local random field strategy, *J. Mater. Chem. C* **8**(11), 3784 (2020).

[43]J. K. Liu, P. Li, C. Y. Li, W. F. Bai, S. T. Wu, P. Zheng, J. J. Zhang and J. W. Zhai, Synergy of a stabilized antiferroelectric phase and domain engineering boosting the energy storage performance of $NaNbO_3$-based relaxor antiferroelectric ceramics, *ACS Appl. Mater. Interfaces* **14**(15), 17662 (2022).

[44]Z. H. Dai, J. L. Xie, W. G. Liu, X. Wang, L. Zhang, Z. J. Zhou, J. L. Li and X. B. Ren, Effective strategy to achieve excellent energy storage properties in lead-free $BaTiO_3$-based bulk ceramics, *ACS Appl. Mater. Interfaces* **12**(27), 30289 (2020).

[45]X. Y. Dong, X. Li, X. L. Chen, J. G. Wu and H. F. Zhou, Simultaneous enhancement of polarization and breakdown strength in lead-free $BaTiO_3$-based ceramics, *Chem. Eng. J.* **409** (2021).

[46]F. H. Pang, X. L. Chen, C. C. Sun, J. P. Shi, X. Li, H. Y. Chen, X. Y. Dong and H. F. Zhou, Ultrahigh energy storage characteristics of sodium niobate-based ceramics by introducing a local random field, *ACS Sustain. Chem. Eng.* **8**(39), 14985 (2020).

[47]P. Shi, X. P. Zhu, X. J. Lou, B. Yang, Q. D. Liu, C. C. Kong, S. Yang, L. Q. He, R. R. Kang and J. T. Zhao, Tailoring ferroelectric polarization and relaxation of BNT-based lead-free relaxors for superior energy storage properties, *Chem. Eng. J.* **428** (2022).

[48]W. J. Shi, Y. L. Yang, L. Y. Zhang, R. Y. Jing, Q. Y. Hu, D. O. Alikin, V. Ya Shur, J. H. Gao, X. Y. Wei and L. Jin, Enhanced energy storage performance of eco-friendly BNT-based relaxor ferroelectric ceramics via polarization mismatch-reestablishment and viscous polymer process, *Ceram. Int.* **48**(5), 6512 (2022).

[49]F. Si, B. Tang, Z. X. Fang, H. Li and S. R. Zhang, A new type of BaTiO3-based ceramics with $Bi(Mg_{1/2}Sn_{1/2})O_3$ modification showing improved energy storage properties and pulsed discharging performances, *J. Alloys Compd.* **819** (2020).

[50]C. C. Sun, X. L. Chen, J. P. Shi, F. H. Pang, X. Y. Dong, H. Y. Chen, K. G. Wang, X. J. Zhou and H. F. Zhou, Simultaneously with large energy density and high efficiency achieved in $NaNbO_3$-based relaxor ferroelectric ceramics, *J. Eur. Ceram. Soc.* **41**(3), 1891 (2021).

[51]H. L. Wang, X. Y. Bu, X. Z. Zhang, P. Zheng, L. L. Li, F. Wen, W. F. Bai, J. J. Zhang, L. Zheng and Y. Zhang, Pb/Bi-free tungsten bronze-based relaxor ferroelectric ceramics with remarkable energy storage performance, *ACS Appl. Energy Mater.* **4**(9), 9066 (2021).

[52]T. Wei, K. Liu, P. Y. Fan, D. J. Lu, B. H. Ye, C. R. Zhou, H. B. Yang, H. Tan, D. Salamon, B. Nan and H. B. Zhang, Novel $NaNbO_3$-$Sr_{0.7}Bi_{0.2}TiO_3$ lead-free dielectric ceramics with excellent energy storage properties, *Ceram. Int.* **47**(3), 3713 (2021).

[53]F. Yang, Z. B. Pan, Z. Q. Ling, D. Hu, J. Ding, P. Li, J. J. Liu and J. W. Zhai, Realizing high comprehensive energy storage performances of BNT-based ceramics for application in pulse power capacitors, *J. Eur. Ceram. Soc.* **41**(4), 2548 (2021).

[54]J. M. Ye, G. S. Wang, M. X. Zhou, N. T. Liu, X. F. Chen, S. Li, F. Cao and X. L. Dong, Excellent comprehensive energy storage properties of novel lead-free $NaNbO_3$-based ceramics for dielectric capacitor applications, *J. Mater. Chem. C* **7**(19), 5639 (2019).

[55]X. Z. Zhang, H. L. Wang, X. Y. Bu, P. Zheng, L. L. Li, F. Wen, W. F. Bai, J. J. Zhang, L. Zheng, J. W. Zhai and Y. Zhang, Simultaneously realizing superior energy storage properties and outstanding charge-discharge performances in tungsten bronze-based ceramic for capacitor applications, *Inorg.Chem.* **60**(9), 6559 (2021).

[56]X. Z. Zhang, P. Zheng, L. Li, F. Wen, W. F. Bai, J. J. Zhang, L. Zheng and Y. Zhang, High energy storage performance in tungsten bronze-based relaxor ceramic via doping with CuO, *Scr. Mater.* **211** (2022).

[57]M. X. Zhou, R. H. Liang, Z. Y. Zhou, S. G. Yan and X. L. Dong, Novel sodium niobate-based lead-free ceramics as new environment-friendly energy storage materials with high energy density, high power density, and excellent stability, *ACS Sustain. Chem. Eng.* **6**(10), 12755 (2018).

[58]J. K. Liu, Y. Q. Ding, C. Y. Li, W. F. Bai, P. Zheng, J. J. Zhang and J. W. Zhai, Relaxor ferroelectric $(Bi_{0.5}Na_{0.5})TiO_3$-based ceramic with remarkable comprehensive energy storage performance under low electric field for capacitor applications, *J. Mater. Sci. Mater. Electron.* **32**(16), 21164 (2021).

[59]M. X. Zhou, R. h. Liang, Z. y. Zhou and X. L. Dong, Novel $BaTiO_3$-based lead-free ceramic capacitors featuring high energy storage density, high power density, and excellent stability, *J. Mater. Chem. C* **6**(31), 8528 (2018).

[60]K. Zhang, P. Zheng, H. F. Zhang, Z. A. Niu, C. Luo, W. F. Bai, J. J. Zhang, L. Zheng and Y. Zhang, Excellent energy storage performance of paraelectric $Ba_{0.4}Sr_{0.6}TiO_3$ based ceramics through induction of polar nano-regions, *Ceram. Int.* **48**(14), 19864 (2022).